1/f noise in graphene nanopores

2015 Nanotechnology 26 074001

(http://iopscience.iop.org/0957-4484/26/7/074001)

IOP Publishing Nanotechnology
Nanotechnology **26** (2015) 074001 (7pp) doi:10.1088/0957-4484/26/7/074001

1/f noise in graphene nanopores

S J Heerema, G F Schneider[1], M Rozemuller, L Vicarelli, H W Zandbergen and C Dekker

Kavli Institute of Nanoscience, Delft University of Technology, Lorentzweg 1, 2628 CJ Delft, The Netherlands

E-mail: c.dekker@tudelft.nl

Received 10 September 2014, revised 3 November 2014
Accepted for publication 7 November 2014
Published 28 January 2015

Abstract

Graphene nanopores are receiving great attention due to their atomically thin membranes and intrinsic electrical properties that appear greatly beneficial for biosensing and DNA sequencing. Here, we present an extensive study of the low-frequency 1/f noise in the ionic current through graphene nanopores and compare it to noise levels in silicon nitride pore currents. We find that the 1/f noise magnitude is very high for graphene nanopores: typically two orders of magnitude higher than for silicon nitride pores. This is a drawback as it significantly lowers the signal-to-noise ratio in DNA translocation experiments. We evaluate possible explanations for these exceptionally high noise levels in graphene pores. From examining the noise for pores of different diameters and at various salt concentrations, we find that in contrast to silicon nitride pores, the 1/f noise in graphene pores does not follow Hooge's relation. In addition, from studying the dependence on the buffer pH, we show that the increased noise cannot be explained by charge fluctuations of chemical groups on the pore rim. Finally, we compare single and bilayer graphene to few-layer and multi-layer graphene and boron nitride (h-BN), and we find that the noise reduces with layer thickness for both materials, which suggests that mechanical fluctuations may be the underlying cause of the high 1/f noise levels in monolayer graphene nanopore devices.

Keywords: graphene, solid-state nanopore, 1/f noise, low-frequency noise, power spectral density

(Some figures may appear in colour only in the online journal)

Introduction

The nanopore field is mainly driven by the demand for a single-molecule DNA sequencing technique that reads DNA bases in a label-free, fast and accurate fashion. Although promising proof-of-principle results have been published using biological pores, such as MspA [1], solid-state nanopores provide some important advantages over biological pores such as stability, adjustable geometry and the ability to integrate into devices [2, 3]. Graphene is a special, advantageous type of solid-state nanopore as it is electrically conducting and atomically thin and therefore potentially provides the capability to reach single-nucleotide resolution in detection. Indeed, various theoretical proposals indicate that its intrinsic electrical properties can be exploited to distinguish different DNA bases [4–12].

In nanopore experiments, charged biomolecules (such as DNA) in an ionic solution are driven through a nanometer-sized hole by an applied transmembrane voltage. The applied bias voltage induces an ion current that prevails due to reversible electrochemical reactions at the electrodes on either side of the membrane. During translocation, the molecule partially blocks the pore, resulting in a temporal change in the ion current, representing the signal. To maximize the signal-to-noise ratio in translocation experiments, any baseline current fluctuations should be minimized; in order to do so, the origin of these fluctuations should be understood. For these reasons, current noise in biological pores, as well as in solid-state nanopores, has been extensively studied [13–19]. Noise studies in graphene nanopores, however, have so far been rare [20].

[1] Current address: Leiden Institute of Chemistry, Supramolecular & Biomaterials Chemistry, Einsteinweg 55, 2333 CC Leiden, The Netherlands.

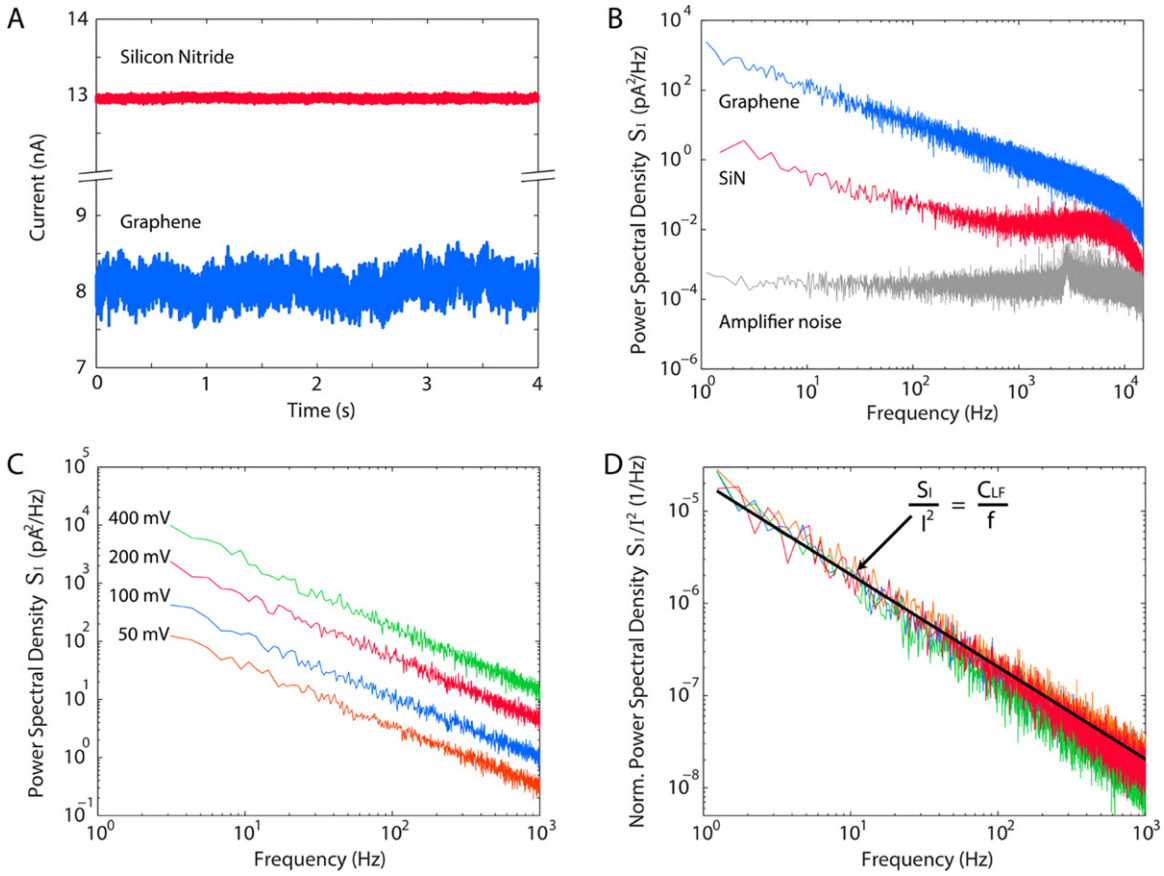

Figure 1. 1/f noise in graphene nanopores and silicon nitride pores. (a) Typical current traces for a graphene pore (R = 12.2 MΩ, d = 10 nm) in blue and a silicon nitride pore (R = 7.8 MΩ, d = 20 nm) in red. The ionic current through the graphene pore shows significant low-frequency variations. (b) Spectral densities of the graphene and silicon nitride pores from panel a. The 1/f frequency in the silicon nitride pore is about two orders of magnitude lower and stretches up to 400 Hz, whereas the graphene pore shows 1/f noise up to the low-pass filter frequency 10 kHz. For presentation, the data were smoothed by calculation of a walking average of 20 data points. (c) Spectral densities at various bias voltages for the same graphene pore. As expected, the curves are bias-voltage dependent. (d) The normalized spectral densities S_I/I^2 collapse onto the same curve. A linear fit of these curves yields the low-frequency noise coefficient C_{LF} that represents the magnitude of the 1/f noise. The curves in panels c and d were smoothed by a walking average of 40 data points.

In order to evaluate the current fluctuations in pore currents, one calculates the current power spectral density S_I, which represents the current power distribution over frequency. Generally, the noise spectrum in nanopore systems is divided into a low-frequency regime (f < ~1 kHz) and a high-frequency regime (f > ~1 kHz), whereas the high-frequency noise power is dominated by the membrane capacitance [21]; the low-frequency noise in solid-state nanopores, as well as in biological nanopores, is characterized by a 1/f dependence [13, 15, 22].

Such low-frequency 1/f noise is a ubiquitous phenomenon, characterised by an inverse dependence of current spectral density on frequency $S_I \sim 1/f^{\gamma}$, where f is the frequency and $\gamma \approx 1$ [23]. Because of its prominent occurrence in most electronic systems (and its implications for their performance), 1/f noise has been profoundly studied over the last few decades. Despite all of these studies, the origin of 1/f noise is still under debate. It is generally accepted that there is not a single physical mechanism that generates this type of noise [24]. Models propose that 1/f noise is related to fluctuations in the number of charge carriers (N), in the mobilities of charge carriers (μ) or in both [25].

Larger currents lead to larger current fluctuations and therefore to higher noise. To obtain a measure for the noise magnitude that can compare the noise levels for various bias conditions, one divides the current power spectral density S_I by the squared current amplitude

$$\frac{S_I}{I^2} = \frac{C_{LF}}{f} \tag{1}$$

where C_{LF} represents the low-frequency noise amplitude. A very commonly used relation in 1/f studies is Hooge's empirical relation $C_{LF} = \frac{\alpha_H}{N}$, which inversely relates the relative noise magnitude C_{LF} to the relevant number of charge carriers N via Hooge's parameter α_H [26]. This model has been shown to provide a fair description of the noise in many different electronic circuits as well as for ionic current systems [27]. Importantly, the relation was also shown to provide a good description for the 1/f noise in silicon nitride nanopores [15].

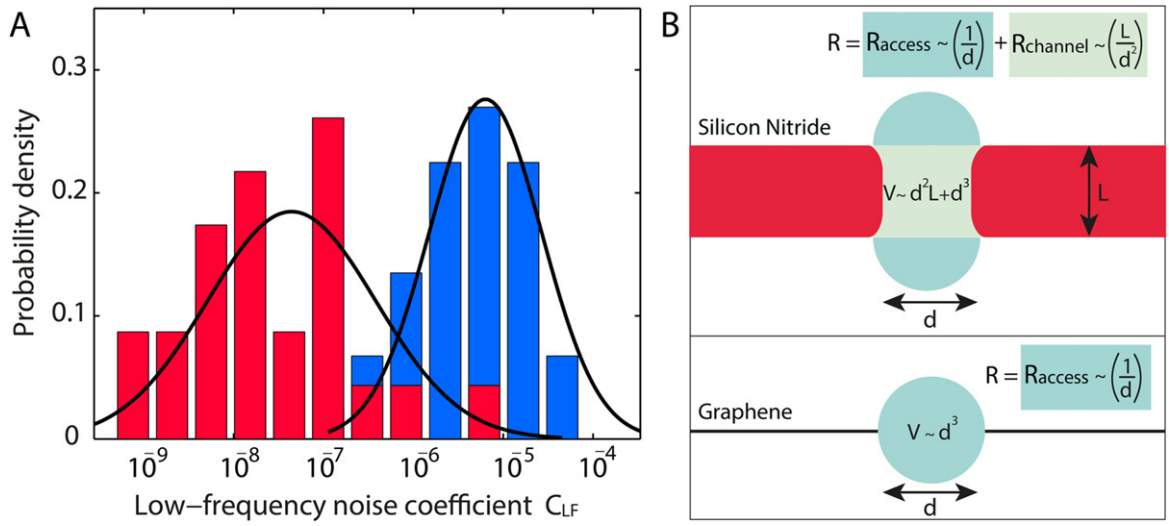

Figure 2. (a) Probability distributions of low-frequency noise coefficients $\boldsymbol{C_{LF}}$ of silicon nitride (red) and graphene nanopores (blue). We compare 24 silicon nitride pores to 45 graphene pores. Linear fits of $\boldsymbol{S_I/I^2}$ are made over the 1/f regimes (for graphene pores this band is 1–1000 Hz; in silicon nitride pores the 1/f regime stretches only up to ~200 Hz, where thermal noise starts to become dominant). We find average values of $\langle \boldsymbol{C_{LF}} \rangle = 4.4 \times 10^{-8}$ for silicon nitride and $\langle \boldsymbol{C_{LF}} \rangle = 6.3 \times 10^{-6}$ for graphene pores, which is a difference of more than two orders of magnitude. All of the measurements are done at 1 M KCl, 10 mM Tris-HCl, pH 8.1. (b) Schematic representation of the geometrical differences between the silicon nitride and graphene nanopores. Expressions for the pore volume V and pore resistance R are indicated.

Here, we discuss the low-frequency noise in graphene nanopores and compare it to noise in silicon nitride pores. We did an extensive study in which we analysed 45 graphene pores, 24 silicon nitride pores and 7 boron nitride pores. We show that the 1/f noise for graphene nanopores is on average two orders of magnitude higher than for silicon nitride pores. We discuss possible explanations for this high 1/f noise in graphene pores. In order to do so, we assess whether Hooge' relation holds by examining the noise properties at various pore sizes and salt concentrations. Additionally, we probe for charged edge interactions by varying the buffer pH. Finally, we discuss the effect of graphene-layer thickness and compare it to that of another layered material: boron nitride.

Results and discussion

Graphene nanopores were fabricated by high-temperature TEM drilling; see Methods. Figure 1(A) provides two typical ionic current traces for a monolayer graphene pore (R = 12.2 MΩ, d = 10 nm) and a silicon nitride pore (R = 7.8 MΩ, d = 20 nm). Both traces are recorded at 100 mV bias voltage and processed in exactly the same way (low-pass filtered with an 8-pole Bessel filter at 10 kHz and smoothed by calculation of the moving average of four data points in logarithmic space). It is very clear that the graphene pore current exhibits pronounced noise in the ionic current. Figure 1(B) shows the corresponding noise spectra, where the current power spectral densities S_I are plotted against frequency in logarithmic space. The noise spectrum of the graphene pore is found to be dominated by a 1/f dependence, extending up to the filter frequency of 10 kHz. Note that, by contrast, the 1/f regime for the silicon nitride pore halts at about 400 Hz, where thermal noise becomes dominant. For reference, we also show the background noise of the amplifier that is recorded at 0 mV. The noise in the graphene pore current is observed to be more than two orders of magnitude higher than that for the silicon nitride current. Figure 1(C) plots the current power spectral densities S_I at varying voltage levels for the same graphene pore. As expected, the noise levels depend on the magnitude of the current, i.e. larger currents lead to higher 1/f noise levels. Indeed, as shown in figure 1(D), the normalised power spectral densities $\left(S_I/I^2\right)$ exhibit the same low-frequency noise magnitude. The 1/f regimes are linearly fitted in logarithmic space, where the fit intercept at 1 Hz $\left(S_I(1\text{Hz})/I^2\right)$ represents the dimensionless low-frequency noise coefficient C_{LF}, which is the magnitude of the pore-specific low-frequency 1/f noise.

With the noise characterization method in place, we can now compare the low-frequency 1/f noise magnitude C_{LF} for a variety of pores and measurement conditions. We compared 45 mono- and bilayer graphene pores to 24 silicon nitride pores. All current traces are recorded at 100 mV at 1 M KCl salt concentration and 10 mM Tris-HCl at pH 8.1. The results of all 1/f noise analyses are presented in the histograms in figure 2(A). The black curves depict log-normal distributions exhibiting an average 1/f coefficient $\langle C_{LF} \rangle = 6.3 \times 10^{-6}$ for graphene pores and an average 1/f coefficient $\langle C_{LF} \rangle = 4.4 \times 10^{-8}$ for silicon nitride pores. On average, the 1/f noise in graphene pores is thus about two orders of magnitude higher than in silicon nitride pores. In logarithmic space, the averages of the distributions are represented as $\log\left(\langle C_{LF} \rangle\right) = -5.2 + -0.6$ for graphene and as $\log\left(\langle C_{LF} \rangle\right) = -7.4 + -0.9$ for silicon nitride. The width of the distribution for the silicon

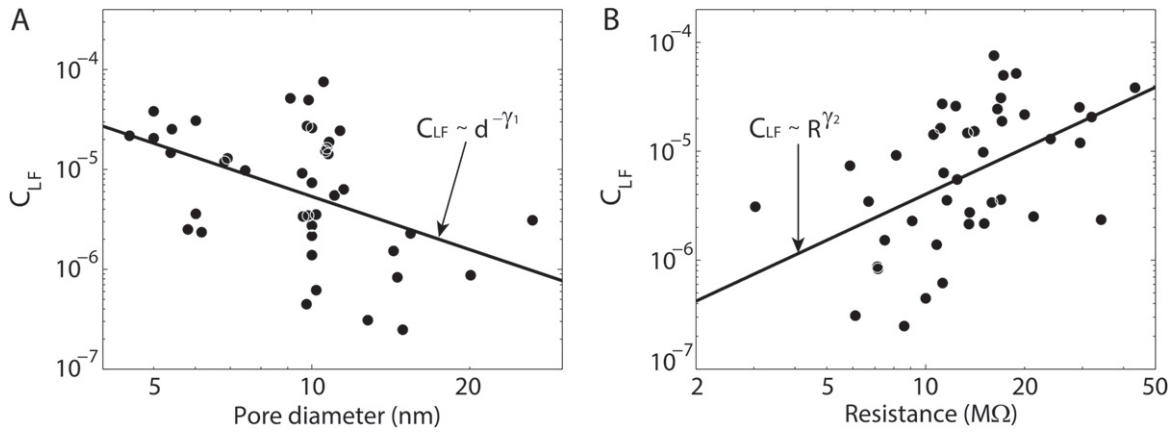

Figure 3. (a) C_{LF} versus pore diameter, plotted double logarithmically. The black line represents a linear fit of the data, yielding $\gamma_1 = 1.8 \pm 0.6$. (b) C_{LF} versus pore resistance in logarithmic space. The linear fit of the data yields $\gamma_2 = 1.4 \pm 0.4$.

nitride samples is larger, which likely is due to a larger variance in pore shape associated with the three-dimensional geometry of the pore.

What explains this significant difference in 1/f noise amplitudes between graphene and silicon nitride nanopores? Conductance fluctuations are most likely caused inside or near the pore as this dominates the circuit's resistance. The geometries of the two different types of pores are sketched in figure 2(B). For silicon nitride pores the resistance can be approximated by $R = \sigma^{-1}\left[\frac{4L}{\pi d^2} + \frac{1}{d}\right]$, where σ represents the bulk conductivity, L is the pore length and d is the pore diameter [28]. The first term represents the pore channel resistance that relates to both the pore length and diameter. The second term denotes the total access resistance that accounts for the convergence of field lines by the pore for both membrane sides [29]. In graphene pores, the resistance is completely dominated by the access resistance $R = \sigma^{-1}\frac{1}{d}$. The relevant pore volume for silicon nitride pores consists of the cylindrical volume d^2L and a term that represents the volumes adjacent to the pore mouths. For each side, this can be regarded to roughly resemble a hemisphere with a size that is set by the pore diameter, located at the centre of the pore mouth. Hence, we consider the effective volume of silicon nitride pores to be determined by $V \sim d^2L + d^3$. For graphene pores the pore length approximates zero, and we thus regard the relevant volume to simply scale as $V \sim d^3$.

We investigated the dependence of the 1/f noise on pore geometry for graphene pores. Figure 3(A) plots the 1/f noise as a function of pore diameter. The diameters are determined from TEM images obtained directly after drilling. Although there is appreciable scatter in the data, there seems to be a correlation between the size and 1/f noise where large pores have lower noise. A linear fit in logarithmic space yields a dependence of $C_{LF} \sim d^{-\gamma_1}$, with $\gamma_1 = 1.8 \pm 0.6$. Additionally, we investigated how the noise scales with the pore resistance, where the resistance values were obtained by linear fitting of recorded IV curves. Figure 3(B) plots the noise coefficients versus resistance in logarithmic space, and a corresponding linear fit yields $C_{LF} \sim R^{\gamma_2}$ with $\gamma_2 = 1.4 \pm 0.4$. The Hooge model predicts that the number of charge carriers N inside of the pore is the important variable, which should be given by the number of ions in the pore volume that determines the resistance. According to Hooge's relation the 1/f noise thus should scale to both the pore diameter and pore resistance with a power law of $\gamma_1 = \gamma_2 = 3$, which is not observed in the data where we observe $\gamma_1 = 1.8 \pm 0.6$ and $\gamma_2 = 1.4 \pm 0.4$.

Another approach to investigate whether the noise amplitude scales inversely with the number of charge carriers in the pore volume is to vary the density of charge carriers by changing the salt level of the buffer. A recent report indeed suggested such a dependence for graphene nanopores [20]. We studied the 1/f noise at salt concentrations between 10 mM and 1 M KCl; see figure 4(A). The grey lines represent results from individual pores with different pore diameters ranging between 4 and 20 nm. 1/f noise levels are seen to slightly increase toward lower salt concentrations. The averages of C_{LF} at 10, 100 and 1000 mM salt are shown in red. Experimentally, we find only a weak dependence of the 1/f noise on salt concentration $\left(C_{LF} \sim N^{-0.27\pm0.02}\right)$. Hooge's relation, however, presented in blue, would predict a much stronger salt dependence $\left(C_{LF} \sim N^{-1}\right)$. Although the noise slightly increases toward lower salt concentrations, our results thus do not follow Hooge's relation.

Next, we examine an alternative explanation for the increased noise levels in graphene nanopores and discuss whether it can be explained by charge fluctuations in the pore rim that would induce noise in the ionic current. To address this, we attempted to modify chemical groups at the pore edge that may switch between a charged and neutral form by varying the pH of the buffer. Carboxyl groups, for example, are expected to be formed at the pore rim and may toggle between their protonated and de-protonated state, with a pKa around 5. We hypothesized that these charge fluctuations may cause an increase in low-frequency noise. To test this, we recorded the currents of individual pores at pH values ranging between pH 1 and 10 at 1 M KCl (figure 4(B)). As before, the grey lines represent measurements of individual pores, and the red line corresponds to their averages. We find that C_{LF} is

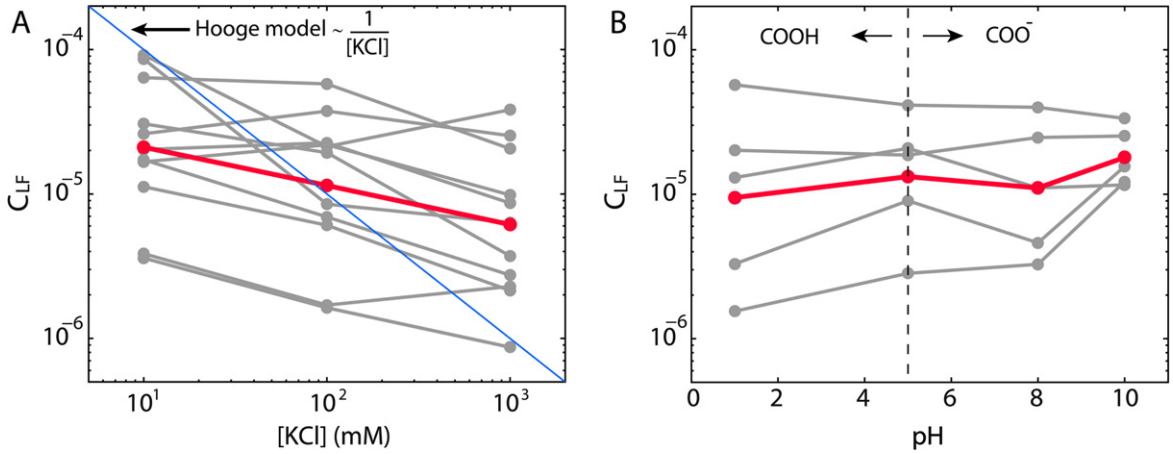

Figure 4. (a) Low-frequency 1/f noise (C_{LF}) dependence on the salt (KCl) concentration. The grey lines represent the results from ten different pores with diameters between 4 and 20 nm. The red line connects the averages of these at 10 mM, 100 mM and 1 M KCl, all at pH 8.1. Although we find a weak trend $(N^{-0.27\pm0.02})$, Hooge's relation is not followed. (b) Low-frequency 1/f noise dependence on pH, measured at pH = 1, 5, 8, 10, for individual pores with pore diameters ranging between 4 and 20 nm. We find no correlation between the pore diameter and 1/f noise dependence on pH. In the case of the toggling of the carboxyl (pKa = 5) between its protonated and de-protonated state, one could expect the noise to peak around pH 5, which is not observed.

unaffected by pH and thus conclude that charge fluctuations due to carboxyl groups at the pore rim do not constitute a dominant source of 1/f noise.

Finally, we studied the noise levels for different membrane thicknesses by comparing the C_{LF} of samples with different layer thicknesses. Several multilayer graphene pores (blue) are compared to the monolayer and bilayer graphene pores (black) in figure 5. An increased number of graphene layers leads to lower noise levels. We augmented the dataset by the inclusion of boron nitride (h-BN) nanopore data. h-BN is structurally very similar to graphene, with boron and nitride in a honeycomb lattice forming a similar sp2 bonded 2-dimensional lattice. We find that the noise in few-layer h-BN is of the same order of magnitude as for graphene pores. For multilayers the noise again reduces strongly: about 1.5 orders of magnitude in going from a monolayer to 20 layers. Such a dependence suggests that mechanical properties of graphene may underlie the noise characteristics, with thinner, more flexible layers yielding more noise than thicker and stiffer layers.

How should the results for the thickness dependence be interpreted? Few-layered graphene and h-BN, like other two-dimensional membranes, are known to be highly flexible [30]. Mechanical resonators of 1–5 micrometer suspended layered materials have been shown to behave in a membrane-like manner for few-layers and in a plate-like manner for multi-layers [31]. This is likely relevant to our nanopore devices, which have free-standing graphene covering a circular hole with a 1 μm diameter. Membrane oscillations can possibly induce fluctuations in the ion flux due to the membrane's movement relative to the ions. In that case, thin 'slack' graphene membranes could induce appreciable low-frequency noise, whereas stiff multilayers would exhibit higher frequency oscillations and less low-frequency conductance fluctuations. Molecular dynamics simulations have shown

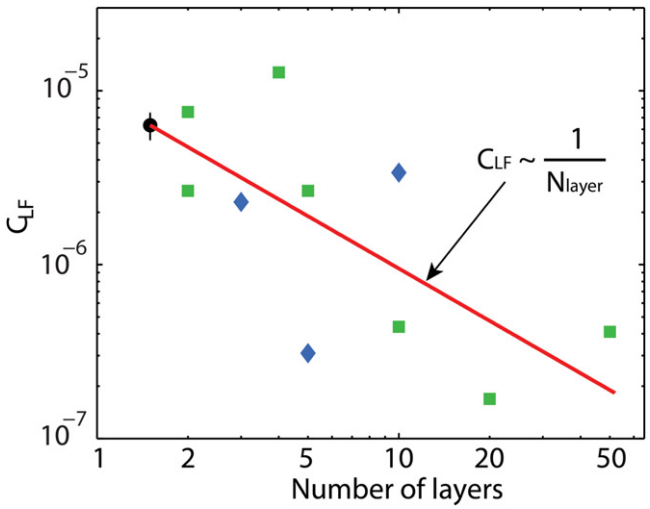

Figure 5. Layer dependence of 1/f noise in graphene and in h-BN nanopores. The black dot represents the mean low frequency coefficient of all monolayer and bilayer graphene nanopores (6.3×10^{-6}). The blue dots (diamonds) yield few-layer graphene pores, showing reduced 1/f noise compared to the mean value of the monolayer and bilayer graphene pores. The noise in few-layer h-BN pores (green squares) is of the same order of magnitude as the few-layer graphene pores. The noise is found to decrease strongly as the layer thickness increases to 20, which is consistent with a $C_{LF} \sim 1/N_{layer}$ dependence (red line). All of the few-layer and multi-layer pores were 10 nm in diameter.

that related to ion bombardment, fluctuations of the graphene membrane may appear close to the pore [32]. Mechanical resonators of layered materials have been shown to have a 1st mode resonance peak in the order of 10 MHz in air [31]. However, such membrane oscillations will be heavily damped due to the water mass that moves along with the membrane. If and in what way such damped oscillations can lead to an increased low-frequency 1/f spectrum remains a subject for

further theoretical studies on the mechanical properties of graphene membranes.

A number of other studies also point in the direction of mechanical fluctuations as the source of the high noise. For example, an experimental study reported that atomic layer deposition (ALD) of several nanometers of titanium oxide reduces the 1/f noise of graphene pores by two orders of magnitude [33]. Similarly, stacked layers of Al_2O_3 and graphene were shown to exhibit lower noise than pure graphene membranes [34]. The disadvantage of such multilayer or stacked structures is that they elude the single-atom layer thickness, which is one of graphene's greatest advantages to potentially measure at single-nucleotide resolution. In another work, it was apparently possible to reduce the 1/f noise by scaling down the area of suspended graphene to 20 nm in diameter, although this was only shown by comparing two individual current traces; it would again point to underlying mechanical fluctuations of the membrane [35].

Conclusion

Here, we have shown that the 1/f noise in monolayer and bilayer graphene nanopores is about two orders of magnitude larger ($\langle C_{LF} \rangle = 6.3 \times 10^{-6}$) than in silicon nitride pores ($\langle C_{LF} \rangle = 4.4 \times 10^{-8}$). In order to explain the high 1/f noise in graphene pores, we studied how it depends on a set of variables. Hooge's model predicts that the 1/f noise is inversely related to the number of charge carriers inside of the pore volume, which was shown to describe the noise in silicon nitride nanopores quite well [15]. Remarkably, we found that the 1/f noise in graphene nanopores does not scale with d^{-3} or R^3, as Hooge's model would predict. An additional study, in which we varied the salt concentration of the buffer, revealed only a weak dependence of the noise on the number of charge carriers ($\sim N^{-0.27}$), which further disproved Hooge's relation in which a N^{-1} dependence is expected. Alternatively, we hypothesized that charge fluctuations due to protonation and de-protonation of carboxyl groups at the pore rim could induce noise. In order to test this, we altered the buffer pH between 1 and 10. However, we found that the pH has no influence on the noise level and concluded that pH-dependent charge fluctuations at the pore edge do not form the dominant source of noise. Finally, we have shown that 1/f noise in graphene and in h-BN pore currents significantly decreases with layer thickness (about 1.5 orders of magnitude in going from a monolayer to 20 layers). We propose that bending fluctuations of the highly flexible graphene or the boron nitride membrane may cause the high 1/f noise in the nanopore current.

In conclusion, we have studied the origin of the significant low-frequency 1/f noise in graphene nanopores and suggest that mechanical fluctuations of the graphene membrane may be the underlying cause. Although this needs to be examined in more detail, it provides a guideline to overcome the high 1/f noise in graphene nanopores and increase signal-to-ratios in further experimental studies, which may accelerate the progress toward a graphene biosensor or sequencer.

Methods

SiN chip fabrication, graphene transfer and TEM drilling

A 200 nm thick platinum heating coil was deposited on a 200 nm low stress silicon nitride layer (LPCVD) on a silicon substrate. Next, a second silicon nitride layer was deposited on top of the platinum coil. After KOH etching a 600×600 micron freestanding SiN membrane was obtained. 1 μm-sized holes were drilled in the silicon nitride membranes with a focussed gallium beam (300 pA) (FEI DualBeam Strata 235).

The monolayer and bilayer graphene flakes were obtained by mechanical exfoliation of natural graphite (NGS Naturgraphit) onto plasma-cleaned (O2, Diener) silicon-silicon oxide wafers (90 nm) (Graphene Supermarket) using adhesive tape (SWT20+, Nitto). An inspection of the monolayer and bilayer graphene was done by optical interference microscopy. The layer thicknesses for few-layered flakes were determined using optical contrast. The multilayer flake thicknesses were determined by AFM measurements. The flakes were transferred onto the micro-fabricated SiN chips according to the wedging transfer technique, described in [36]. The flakes were transferred onto the silicon nitride membranes. The same procedure was followed for boron nitride pore fabrication.

The nanopores were drilled using a FEI Titan 80–300 in STEM mode, operating at an acceleration voltage of 300 kV with a beam diameter of 0.1 nm and a beam current of 0.15 nA. Importantly, the graphene was heated at 600 °C in order to prevent carbon contamination on the surface and to maintain the crystalline structure up to the pore edge; in order to do so a 10 mA current was passed through the platinum heating coil [37]. Pore diameters varied between 4 and 30 nm and were measured from the TEM images obtained right after drilling.

The SiN pores were fabricated as described previously [38].

Current recording

The chips were cleaned with ethanol and subsequently mounted in a polyether ether ketone (PEEK) flowcell separating two aqueous chambers into which Ag/AgCl electrodes were inserted. The buffers contained 1 M KCl solution, 10 mM Tris-HCl, pH 8.1 at room temperature. The buffers for the pH measurements contained 1 M KCl and 55 mM HCl (pH = 1), 0.4 mM NaAc and 4 μM AcAc (pH = 5) and 1.6 mM NaOH (pH = 10) (Sigma-Aldrich). All of the currents were recorded in the absence of DNA in the chambers. Ionic currents were detected using an Axopatch 200B amplifier at a 100 kHz bandwidth and digitized with a DAQ card at 500 kHz. The current traces were filtered using an 8-pole Bessel filter at 10 kHz in Clampfit.

Data analysis

Power spectral densities were calculated by taking the Fourier transform of the autocorrelation function and dividing it by the sampling frequency and the sample length. For

normalization, the power spectral densities were divided by the mean current of the corresponding traces. In general, the 1/f noise was fitted from 1–1000 Hz for graphene pores and between 1–200 Hz for silicon nitride pores. For data presentation, the curves were smoothed by calculation of a walking average of 4–40 of the nearest neighbour points. All of the analyses and fitting were done in Matlab.

Acknowledgments

We would like to thank Meng-Yue Wu for the TEM drilling and imaging of the silicon nitride nanopores. We acknowledge the funding received from the Netherlands Organisation for Scientific Research (NWO/OCW), the European Research Council (starting grant no. GA 256270) and The European Union Seventh Framework Programme under grant agreement no. 604391, Graphene Flagship.

References

[1] Laszlo A H *et al* 2014 Decoding long nanopore sequencing reads of natural DNA *Nature Biotech.* **32** 829–33
[2] Dekker C 2007 Solid-state nanopores *Nat. Nanotechnol* **2** 209–15
[3] Schneider G F and Dekker C 2012 DNA sequencing with nanopores *Nat. Biotechnol.* **30** 326–8
[4] Postma H W C 2010 Rapid sequencing of individual DNA molecules in graphene nanogaps *Nano Lett.* **10** 420–5
[5] Nelson T, Zhang B and Prezhdo O V 2010 Detection of nucleic acids with graphene nanopores: ab initio characterization of a novel sequencing device *Nano Lett.* **10** 3237–42
[6] Min S K, Kim W Y, Cho Y and Kim K S 2011 Fast DNA sequencing with a graphene-based nanochannel device *Nat. Nanotechnol.* **6** 162–5
[7] Avdoshenko S M, Nozaki D, Gomes da Rocha C, González J W, Lee M H, Gutierrez R and Cuniberti G 2013 Dynamic and electronic transport properties of DNA translocation through graphene nanopores *Nano Lett.* **13** 1969–76
[8] Saha K K, Drndić M and Nikolić B K 2012 DNA base-specific modulation of microampere transverse edge currents through a metallic graphene nanoribbon with a nanopore *Nano Lett.* **12** 50–5
[9] Wells D B, Belkin M, Comer J and Aksimentiev A 2012 Assessing graphene nanopores for sequencing DNA *Nano Lett.* **12** 4117–23
[10] Prasongkit J, Grigoriev A, Pathak B, Ahuja R and Scheicher R H 2011 Transverse conductance of DNA nucleotides in a graphene nanogap from first principles *Nano Lett.* **11** 1941–5
[11] Girdhar A, Sathe C, Schulten K and Leburton J-P 2013 Graphene quantum point contact transistor for DNA sensing *Proc. Natl. Acad. Sci. USA* **110** 16748–53
[12] Qiu W and Skafidas E 2014 Graphene nanopore field effect transistors *J. Appl. Phys.* **116** 023709
[13] Bezrukov I and Vodyannoy S M 1994 Noise in biological membranes and relevant ionic systems *Biomembr. Electrochem.* **235** 375–99
[14] Wohnsland F and Benz R 1997 1/f -Noise of open bacterial porin channels *J. Membr. Biol.* **158** 77–85
[15] Smeets R M M, Keyser U F, Dekker N H and Dekker C 2008 Noise in solid-state nanopores *Proc. Natl. Acad. Sci. USA* **105** 417–21
[16] Smeets R M M, Dekker N H and Dekker C 2009 Low-frequency noise in solid-state nanopores *Nanotechnology* **20** 095501
[17] Hoogerheide D P, Garaj S and Golovchenko J A 2009 Probing surface charge fluctuations with solid-state nanopores *Phys. Rev. Lett.* **102** 256804
[18] Powell M R, Vlassiouk I, Martens C and Siwy Z S 2009 Nonequilibrium 1/f noise in rectifying nanopores *Phys. Rev. Lett.* **103** 248104
[19] Powell M R, Sa N, Davenport M, Healy K, Vlassiouk I, Létant S E, Baker L A and Siwy Z S 2011 Noise properties of rectifying nanopores *J. Phys. Chem.* C **115** 8775–83
[20] Kumar A, Park K-B, Kim H-M and Kim K-B 2013 Noise and its reduction in graphene based nanopore devices *Nanotechnology* **24** 495503
[21] Rosenstein J K, Wanunu M, Merchant C A, Drndic M and Shepard K L 2012 Integrated nanopore sensing platform with sub-microsecond temporal resolution *Nat. Methods* **9** 487–92
[22] Chen P, Mitsui T, Farmer D B, Golovchenko J, Gordon R G and Branton D 2004 Atomic layer deposition to fine-tune the surface properties and diameters of fabricated nanopores *Nano Lett.* **4** 1333–7
[23] Johnson J 1925 The Schottky effect in low frequency circuits *Phys. Rev.* **26** 71–85
[24] Hooge F N 1994 1/f noise sources *IEEE Trans. Electron Devices* **41** 1926–35
[25] Balandin A A 2013 Low-frequency 1/f noise in graphene devices *Nat. Nanotechnol.* **8** 549–55
[26] Hooge F N 1969 1/*f* noise is no surface effect *Phys. Lett.* A **29** 139–40
[27] Hooge F N 1970 noise in the conductance of ions in aqueous solutions *Phys. Lett.* A **33** 169–70
[28] Kowalczyk S W, Grosberg A Y, Rabin Y and Dekker C 2011 Modeling the conductance and DNA blockade of solid-state nanopores *Nanotechnology* **22** 315101
[29] Hall J E 1975 Access resistance of a small circular pore *J. Gen. Physiol.* **66** 531–2
[30] Lee C, Wei X, Kysar J W and Hone J 2008 Measurement of the elastic properties and intrinsic strength of monolayer graphene *Science* **321** 385–8
[31] Castellanos-Gomez A, van Leeuwen R, Buscema M, van der Zant H S J, Steele G A and Venstra W J 2013 Single-layer MoS(2) mechanical resonators *Adv. Mater.* **25** 6719–23
[32] Sathe C, Zou X, Leburton J-P and Schulten K 2011 Computational investigation of DNA detection using graphene nanopores *ACS Nano* **5** 8842–51
[33] Merchant C A *et al* 2010 DNA translocation through graphene nanopores *Nano Lett.* **10** 2915–21
[34] Venkatesan B M, Estrada D, Banerjee S, Jin X, Dorgan V E, Bae M-H, Aluru N R, Pop E and Bashir R 2012 Stacked graphene-Al2O3 nanopore sensors for sensitive detection of DNA and DNA-protein complexes *ACS Nano* **6** 441–50
[35] Garaj S, Liu S, Golovchenko J A and Branton D 2013 Molecule-hugging graphene nanopores *Proc. Natl. Acad. Sci. USA* **110** 12192–6
[36] Schneider G F, Calado V E, Zandbergen H, Vandersypen L M K V and Dekker C 2010 Wedging transfer of nanostructures *Nano Lett.* **10** 1912–6
[37] Song B, Schneider G F, Xu Q, Pandraud G, Dekker C and Zandbergen H 2011 Atomic-scale electron-beam sculpting of near-defect-free graphene nanostructures *Nano Lett.* **11** 2247–50
[38] Janssen X J A, Jonsson M P, Plesa C, Soni G V, Dekker C and Dekker N H 2012 Rapid manufacturing of low-noise membranes for nanopore sensors by trans-chip illumination lithography *Nanotechnology* **23** 475302